DOI: 10.2478/v10077-012-0003-6

Paweł Grzegorz Kossakowski

Kielce University of Technology, Faculty of Civil and Environmental Engineering, Chair of Strength of Materials and Concrete Structures, Al. Tysiąclecia Państwa Polskiego 7, 25-314 Kielce, Poland,
kossak@tu.kielce.pl

THE ANALYSIS OF INFLUENCE OF TVERGAARD'S PARAMETERS ON S235JR STEEL RESPONSE IN HIGH STRESS TRIAXIALITY

ABSTRACT

The influence of Tvergaard's parameters q_i of Gurson-Tvergaard-Needleman (GTN) material model on S235JR steel response was considered in the study. The analysis concerns the strength curves simulated numerically for notched tensile elements under static tension in complex stress state defined by high initial stress triaxiality $\sigma_m/\sigma_e > 1$. Typical and material-dependent values of Tvergaard's parameters q_i were examined. The influence of the Tvergaard's parameters q_i on material response was noticed at the failure range for S235JR steel in the case of high stress triaxiality.

Key words: *Tvergaard's parameters, Gurson-Tvergaard-Needleman material model, GTN, high stress triaxiality, S235JR steel*

INTRODUCTION

The Gurson-Tvergaard-Needleman (GTN) material model is one of an advanced damage models, which takes into consideration the influence of micro-defects on the material strength. Due to significant applicability of the GTN material model in strength analyses, this model is implemented in computational programs used in engineering. For instance, according to the current standards obligatory in European Union such as PN-EN 1993-1-10 [1] and its commentary by Sedlacek et al. [2], the GTN material model is recommended for use in analyses of pre-failure condition for building structures. This model allows us to conduct complete analysis of the load-bearing capacity of the structure up to the total failure of the material and elements and ensures good consistency of the results obtained numerically and experimentally (eg. [3-6]).

Taking this into consideration above, a research was undertaken to develop the procedure which allow to simulate numerically the load-bearing capacity of building structural elements made of S235JR steel basing on the GTN material model. Due to the problems encountered in engineering application of this model, especially the lack of the microstructural GTN parameters for steel grades used in civil engineering, the standardisation of these parameters is one of the most important problems to solve.

The analysis of Tvergaard's parameters q_i, some of the fundamental constants in GTN material model, is presented in the study. The elements under static tension in complex stress state defined by initial stress triaxiality $\sigma_m/\sigma_e > 1$, where σ_m and σ_e denotes the mean and

effective stress, respectively, were considered. The analysis was performed for S235JR steel, popular steel grade used in technique, especially in the building. Therefore it seems, that obtained results may have practical significance in engineering problems.

GTN MATERIAL MODEL AND TVERGAARD'S PARAMETERS

The Gurson-Tvergaard-Needleman (GTN) material model is based on the original Gurson material for a porous solid [7], where the influence of the micro-defects on the material was defined by the increase in the void volume fraction f included in classical Huber-Mises-Hencky criterion. The Gurson model was modified by Tvergaard [8], which introduced so-called Tvergaard's parameters q_i, defining selected microstructural parameters and plastic properties of the material. Taking into consideration the further modifications by Tvergaard and Needleman [9] and Needleman and Tvergaard [10], the modified GTN material model is described by following yield criterion

$$\Phi = \left(\frac{\sigma_e}{\sigma_0}\right)^2 + 2q_1 f^* \cosh\left(q_2 \frac{\sigma_{kk}}{2\sigma_0}\right) - \left(1 + q_3 f^{*2}\right) = 0 \tag{1}$$

where: σ_e – effective stress, σ_0 – yield stress, σ_{kk} – first invariant of the stress state, f^* – actual void volume fraction, q_i – Tvergaard's parameters.

The GTN yield criterion (1) is described by many microstructural constants, including Tvergaard's parameters q_i, which have influence on the material strength, discussed below basing on the results and information presented by Cordigliano et. al [11].

The yield domain (1) is affected by first Tvergaard's parameter q_1, which modifies the actual void volume fraction f^*. The plastic limit is encountered for reduced stress conditions when $q_1 > 1.0$ (Fig. 1a). Higher values of parameter q_1 decrease the strength of the GTN material. The stress-strain relation $\sigma(\varepsilon)$ is influenced by parameter q_1 modifying the stress carrying capacity, which reveal the softening due to void growth dominating over hardening properties of the matrix material.

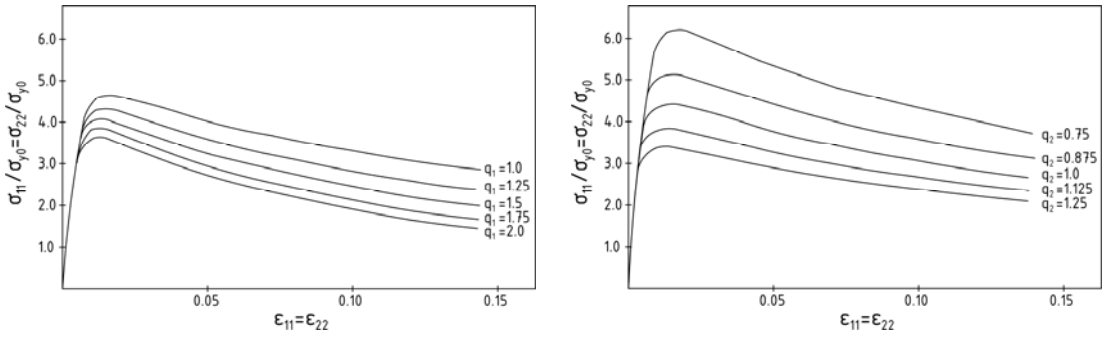

Fig. 1. Effects of Tvergaard's parameters on the nonlinear response of the GTN constitutive law at $\varepsilon_{22}/\varepsilon_{11} = 1.0$ for: a) $1.0 \le q_1 \le 2.0$; b) $0.75 \le q_2 \le 1.25$ [11]

For higher values of q_1 the stronger softening of the material is observed (Fig. 1a). The value of $q_1 = 1.5$ was proposed by Tvergaard [8] as optimal to model numerically the localization of

plastic deformations effect and fracture phenomena for many porous solids, including metals.

The second Tvergaard's parameter q_2 modifies first invariant of the stress state σ_{kk} being a function of the hydro-static component $\sigma_m = \sigma_{kk}/3$. For high values of q_2 the yield limit is strongly reduced. According to Tvergaard's results [12] the suggested value was determined as $q_2 = 1.0$. High values of q_2 lead to the strong softening due to the void growth, revealing the annihilation of the strain hardening properties of the matrix material (Fig. 1b). Then overall strength properties of the porous GTN material are reduced.

As concluded, typical and suggested values of Tvergaard's parameters for steel grades were established as $q_1 = 1.5$, $q_2 = 1.0$ and $q_3 = q_1^2 = 2.25$.

Above values of Tvergaard's parameters have been treated as constant for many years. Further studies, including the analysis performed by Faleskog et. al [13] show a dependence of Tvergaard's parameters on the material properties. As can be seen in Figure 2, the values of q_1 and q_2 parameters are related to the elastic-plastic properties of the material, defined by strain hardening exponent N and yield stress σ_0 to modulus of elasticity E ratio.

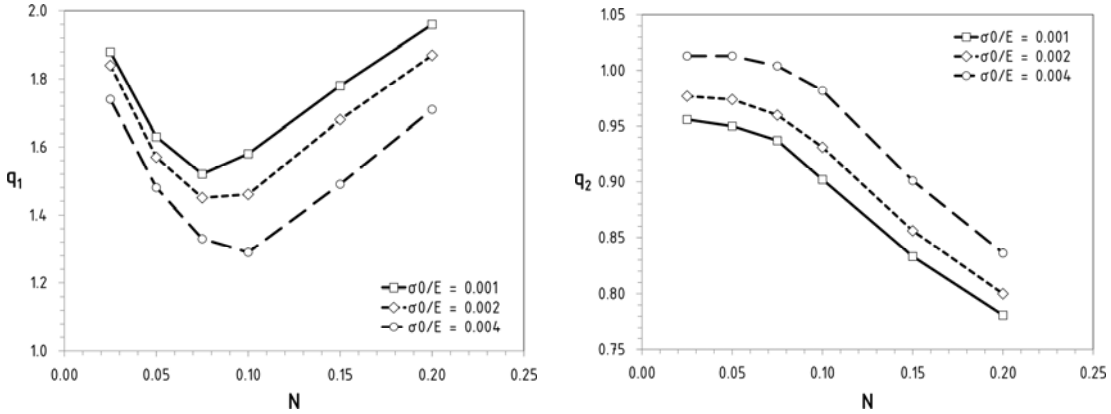

a) b)

Fig. 2. The changes of q_1 (a) and q_2 (b) depending on strain hardening N, for different σ_0/E ratios [13]

TVERGAARD'S PARAMETERS OF GTN MATERIAL MODEL FOR S235JR STEEL

As mentioned at the beginning, the analysis of Tvergaard's parameters which are some of the basic GTN material constants is presented in this study for S235JR steel. The analysis of the influence of typical and material-dependent values of Tvergaard's parameters on the S235JR steel response in the case of complex stress state defined by high initial stress triaxiality $\sigma_m/\sigma_e > 1$ is the main issue.

In order to determine Tvergaard's parameters for S235JR steel the static tensile tests were performed according to [14], which allow to determine basic strength properties of tested material. According to the results obtained, the average strength parameters were as follows: the yield stress $\sigma_0 = 318$MPa, the tensile strength $R_m = 446$MPa, and the displacement percentage $A_5 = 33.9\%$ [3]. Basing on the strength curves $\sigma(\varepsilon)$ determined during the tests, the elastic-plastic model of S235JR steel used in further simulations was elaborated.

Two sets of Tvergaard's parameters for S235JR steel were considered in the study. Typical and suggested values of Tvergaard's parameters for construction steel grades were assumed in the first set as follows

$$q_i = \begin{cases} q_1 = 1.5 \\ q_2 = 1.0 \\ q_3 = q_1^2 = 2.25 \end{cases} \tag{2}$$

The second set of Tvergaard's parameters included their values determined using the results of Faleskog et al. [13], based on relations with the strength properties of S235JR steel, i.e. the yield stress $\sigma_0 = 318$MPa, the modulus of elasticity E = 205 GPa and the strain-hardening exponent N = 0.183. For the ratio of σ_0/E = 0.00155 and N = 0.183 material-dependent Tvergaard's parameters were established using the relationships shown in the Figure 2 as

$$q_i = \begin{cases} q_1 = 1.90 \\ q_2 = 0.81 \\ q_3 = q_1^2 = 3.61 \end{cases} \tag{3}$$

Finally the GTN model parameters for S235JR steel were assumed. Taking into consideration the results of microstructural examinations [3], the average initial void volume fraction f_0 was established. Other GTN material parameters was determined basing on the results of combined experimental-numerical method presented by Kossakowski [3-6]. The standard tensile tests were simulated numerically using a Finite Element Method program Abaqus version 6.10. The GTN material model parameters were changed iteratively within certain limits basing in the convergence of the $\sigma(\varepsilon)$ values obtained numerically and experimentally. The GTN parameters determined for S235JR steel are summarized in Table 1.

Table 1. *Microstructural parameters of GTN material model of S235JR steel*

Model No.	f_0	f_c	f_F	q_1	q_2	q_3	ε_N	f_N	s_N
1	0.001	0.06	0.667	1.50	1.00	2.25	0.3	0.04	0.05
2	0.001	0.06	0.667	1.90	0.81	3.61	0.3	0.04	0.05

THE ANALYSIS OF TVERGAARD'S PARAMETERS FOR S235JR STEEL

The analysis of the influence of Tvergaard's parameters q_i on the S235JR steel response was performed using a circular cross-sectional elements with a circumferential annular notch subjected to static tension with displacement control increase, which were tested experimentally and modelled during numerical simulations.

A research presented in the paper was performed taking into consideration the results of wide research program [3-6] focused on the tensile elements with circular cross-sections for different notch radii. The effects observed during this studies were most intense for elements with a stress triaxiality above unity, therefore the analysis was performed for such elements.

Here the elements with diameter of $2R_0$ =14.0 mm and $2r_0$ = 7.0 mm and the notch radius ρ_0 = 1.0 mm (Fig. 3) were considered, which allowed to obtain a complex state of stress corresponding to the initial stress triaxiality σ_m/σ_e = 1.345. During the static tensile tests the

load F and displacement of points distributed symmetrically along the notch l, were measured with the extensometer of the initial length of 32.56mm.

The numerical simulations of tensile strength tests of notched elements were fundamental part of the analysis performed on Tvergaard's parameters of S235JR steel in high stress triaxiality. Abaqus version 6.10 Finite Element Method-based program was applied with using the Dynamic Explicit module [15].

The numerical models were built on the basis of the geometry of the notched specimens used during experimental tests as a circular cross sectional bars with an ring notch radius ρ_0 = 1.0 mm. They were subjected to the static tension at a controlled rate of displacement 4mm/min, similarly as in the experiments. Only half of the samples were modelled due to the symmetry of the problem, using standard axisymmetric CAX4R elements [15]. During simulations the modified Gurson-Tvergaard-Needleman material model was applied for numerical models, according to the GTN parameters summarized in Table 1.

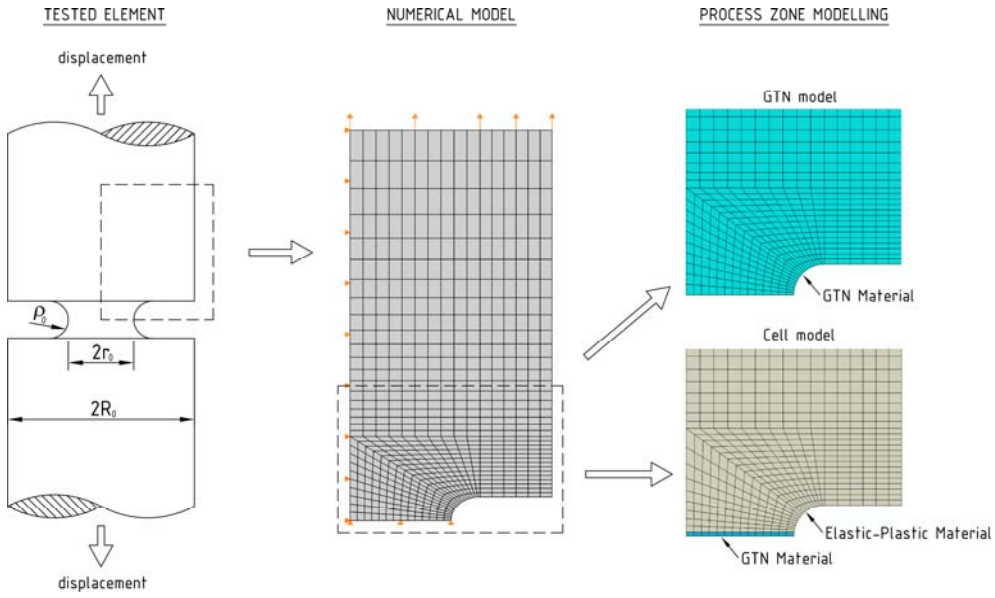

Fig. 3. Scheme of tested element and numerical models

As can be seen on Figure 3, two general models were applied during the numerical modelling of the tensile elements, according to the recommendations for simulations with using damage material models.

The non-local approach was applied for the numerical model referred as *GTN*. The modified GTN material model was assumed for whole numerical model, in consequence, the porous material was applied for whole material. When the local approach was applied, referred as *Cell*, the modified GTN material was assumed only for the elements in the region near to the crack plane, i.e. process zone. For the rest of the numerical model the elastic-plastic material model was assumed.

The mesh size of the process zone was based on the microstructurally-based length scales method, which defines the characteristic length l_c, necessary to take into account in the meshing process for minimal cell dimensions. The characteristic length l_c was determined for S235JR steel during the microstructural examinations as the dimensions of plateaus and valleys measured on the fracture surface, using the results reported in [5]. The average value of l_c was established as $l_c \approx 250\mu m$. The region of the process zone was meshed basing on the mesh size equal to $D \times D/2$, where $D = l_c = 250\mu m$.

The analysis of Tvergaard's parameters for S235JR steel in high stress triaxiality was performed basing on two sets of GTN material parameters summarized in Table 1 using values of q_i defined by (2) and (3) for *GTN* and *Cell* numerical models. The material response was examined by analysis of the force-elongation $F(l)$ curves determined experimentally and numerically, as presented in Figure 4.

First of all it should be noted, that the tensile strength curves were consistent in the middle range of deformation, when the maximum force F was reached for results of experiments and numerical simulations using both *GTN* and *Cell* models. At this range the differences in values of forces were insignificant. Above the maximum force up to the material failure, the differences in strength curves $F(l)$ revealed, depending on the numerical model and Tvergaard's parameters assumed, which is presented below.

When *GTN* model was applied, the slight softening effect revealed in the range of elongation $l > 0.5$ mm up to total failure of the material, the forces F determined numerically were lower than those obtained during experiments (Fig. 4a). The forces obtained by using typical Tvergaard's parameters, i.e. $q_1 = 1.5$, $q_2 = 1.0$, $q_3 = 2.25$, were lower than those using material-dependent Tvergaard's parameters, i.e. $q_1 = 1.90$, $q_2 = 0.81$, $q_3 = 3.61$. This relation was noticed above maximum force up to the material failure. The maximum difference in forces obtained by using assumed Tvergaard's parameters was 14.6% at the failure moment.

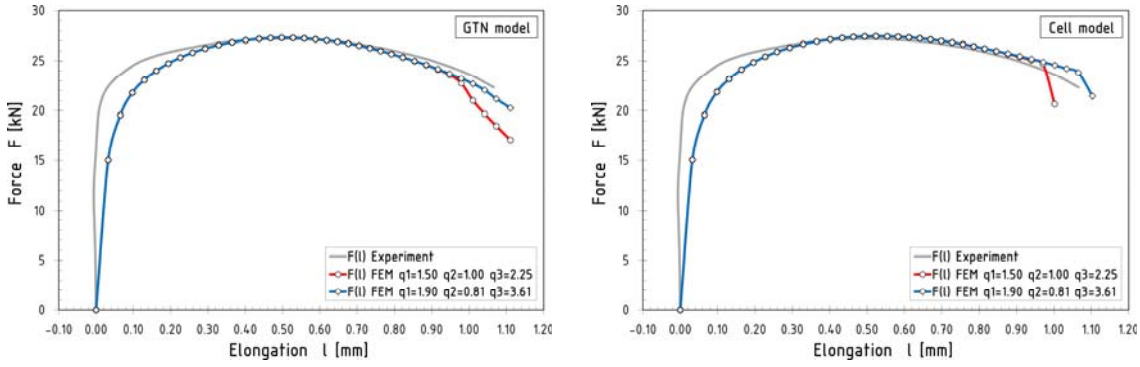

a) b)

Fig. 4. Force-elongation $F(l)$ curves determined experimentally and numerically for: a) *GTN* model; b) *Cell* model

In the case of *Cell* model application, the softening effect was not observed, but the reverse phenomenon was noticed. In the range of elongation $l > 0.52$ mm the forces F determined numerically were higher than those determined experimentally. In the range above the maximum force, similarly to *GTN* model, the forces obtained by using typical Tvergaard's parameters were lower than those using material-dependent Tvergaard's parameters, but the difference in forces was higher, 75.7%. As can be seen on Figure 4 b, when *Cell* mode was applied, the failure moment was strongly connected with Tvergaard's parameters. When typical Tvergaard's parameters were applied, the failure moment was observed visible earlier than for material-dependent walues of q_i.

In the next part of the examinations the analysis of changes of void volume fraction *VVF* parameters was performed. Taking into account that the void volume fraction is higher in the middle of the element at the failure moment in comparison to the external parts, the fracture is expected in the middle of the sample. The changes of the *VVF* parameter for a point in the middle of the fracture plane, on the axis of the element are shown in Figure 5.

As can be seen, for both numerical models applied, i.e. *GTN* and *Cell*, the voids begin to increase earlier when typical values of Tvergaard's parameters, i.e. $q_1 = 1.5$, $q_2 = 1.0$, $q_3 =$

2.25, were used in comparison to than those using material-dependent values of q_i, i.e. q_1 = 1.90, q_2 = 0.81, q_3 = 3.61, at the range above maximum force up to the material failure.

When *GTN* model was applied the beginning of the void growth was observed for elongation about l = 8.0mm, while for *Cell* model this phenomenon was noticed slightly later, for elongation about l = 9.0mm. For typical values of q_i the increase of the *VVF* parameter was much rapid in comparison to the material-dependent values of q_i. It can be concluded, that Tvergaard's parameters affected significantly the void growth in analysed situation.

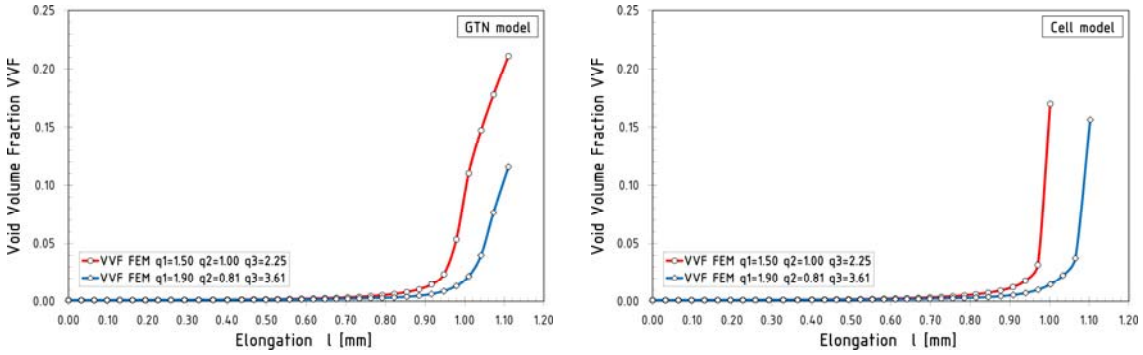

a) b)

Fig. 5. Void Volume Fraction *VVF* curves determined experimentally and numerically using: a) *GTN* model; b) *Cell* model

As can be seen at the failure moment, the *VVF* parameters were significantly higher for typical values of q_i, in comparison to than those using material-dependent values, for both numerical models applied. The maximum difference in *VVF* parameter was observed as 232% when *GTN* model was applied.

When *Cell* model was used, the differences in *VVF* parameter at the failure were even more, but taking into consideration that the material failed suddenly in this case, the moment of failure is an interesting phenomenon. When typical values of q_i were assumed, the failure moment was observed for elongation about l = 1.0 mm, while for material-based q_i this moment was noticed for l = 1.1 mm.

DISCUSSION AND CONCLUSIONS

As presented above, the several characteristic phenomena were observed during analysis performed.

The tensile strength curves determined experimentally and numerically were consistent in the middle range of deformation. At the text range, above the maximum force up to the material failure, the differences in strength curves $F(l)$ revealed, depending on the numerical model and the Tvergaard's parameters assumed. When *GTN* model was applied, a slight softening effect revealed, forces F determined numerically were lower than those obtained numerically, while for *Cell* model the reverse phenomenon was noticed.

The influence of Tvergaard's parameters on S235JR steel response was the most important effect observed in the case of high initial stress triaxality at the range from maximum force up to the material failure. For both non-local and local approaches, i.e. *GTN* and *Cell* model applied, respectively, the forces obtained by using typical Tveergard's parameters, i.e. q_1 =

1.5, q_2 = 1.0, q_3 = 2.25, were lower than those using material-dependent Tveergard's parameters, i.e. q_1 = 1.90, q_2 = 0.81, q_3 = 3.61. It should be noticed also, that Tvergaard's parameters affected the failure moment when *Cell* model was used, when typical Tvergaard's parameters were applied, the failure moment was observed visible earlier than for material-dependent values of q_i.

These phenomena were closely related to the void growth observed during deformation process. For both numerical models applied, i.e. *GTN* and *Cell*, the voids began to increase earlier when typical values of Tvergaard's parameters, i.e. q_1 = 1.5, q_2 = 1.0, q_3 = 2.25, were used in comparison to than those using material-dependent values of q_i, i.e. q_1 = 1.90, q_2 = 0.81, q_3 = 3.61, at the range above maximum force up to the material failure. At the failure moment, the values of *VVF* parameters were significantly higher for typical values of q_i, in comparison to the material-dependent values of q_i. For local approach, when *Cell* model was applied, the differences in *VVF* parameter at the failure were even more than for non-local approach, i.e. *GTN* model, for assumed values of Tvergaard's parameters. When *Cell* model was used, the failure moment was observed visible earlier in comparison to the *GTN* model, due to the much rapid and intensive void growth.

Summing up, the influence of Tvergaard's parameters on S235JR steel response was noticed in the case of high initial stress triaxality, affecting the strength curves $F(l)$ due to void growth at the range from maximum force up to the material failure.

Basing on the results of analysis performed on the Tvergaard's parameters for S235JR steel in high stress triaxiality, the following conclusions have been drawn:

1. The tensile strength curves determined experimentally and numerically basing on the non-local (*GTN* model) and local (*Cell* model) approach were consistent in the middle range of deformation, when the maximum force F was reached. At this range the differences in values of forces were insignificant. Above the maximum force up to the material failure, the differences in strength curves $F(l)$ revealed, depending on the numerical model and Tvergaard's parameters assumed.
2. When *GTN* model was applied, the slight softening effect revealed in the range above maximum force up to a total failure of the material, when forces determined numerically were lower than those obtained during experiments. The reverse phenomenon was noticed in the case of *Cell* model application.
3. For the both *GTN* and *Cell* numerical models, the visible influence of Tvergaard's parameters on the S235JR steel response was noticed at the range from maximum force up to the material failure in the case of high stress triaxiality. The forces obtained by using typical Tvergaard's parameters, i.e. q_1 = 1.5, q_2 = 1.0, q_3 = 2.25, were lower than those using material-dependent Tvergaard's parameters, i.e. q_1 = 1.90, q_2 = 0.81, q_3 = 3.61.
4. Tvergaard's parameters affected significantly the void growth which corresponds to the response of S235JR in high stress triaxiality. For both numerical models applied, i.e. *GTN* and *Cell*, the voids began to increase earlier when typical values of Tvergaard's parameters, i.e. q_1 = 1.5, q_2 = 1.0, q_3 = 2.25, were used in comparison to than those using material-dependent values of q_i, i.e. q_1 = 1.90, q_2 = 0.81, q_3 = 3.61, at the range above maximum force up to the material failure.
5. When *Cell* mode was applied, the failure moment was strongly related to Tvergaard's parameters. When typical Tvergaard's parameters were applied, the failure moment was observed visible earlier than for material-dependent values of q_i.

REFERENCES

1. PN-EN 1993-1-10:2005 Eurocode 3 - Design of Steel Structures - Material Toughness and Through-thickness Properties.
2. Sedlacek G., Feldmann M., Kühn B., Tschickardt D., Höhler S., Müller C., Hensen W., Stranghöner N., Dahl W., Langenberg P., Münstermann S., Brozetti J., Raoul J., Pope R., Bijlaard F.: Commentary and Worked Examples to EN 1993-1-10 "Material toughness and through thickness properties" and other toughness oriented rules in EN 1993, JRC Scientific and Technical Reports, European Commission Joint Research Centre, 2008.
3. Kossakowski P.G: An analysis of the load-carrying capacity of elements subjected to complex stress states with a focus on the microstructural failure. Archives of Civil and Mechanical Engineering 10 (2010), pp. 15-39.
4. Kossakowski P., Trąmpczyński W.: Numerical simulation of damage of steel S235JR including the influence of microstructural damage. Mechanical Review (Przegląd Mechaniczny) 4 (2011) (in Polish), p. 15-22.
5. Simulation of ductile fracture of S235JR steel using computational cells with microstructurally-based length scales. Journal of Theoretical and Applied Mechanics 50 (2012), pp. 589-607.
6. Kossakowski P.: Simulation of the plastic range work of structural steel in a complex stress state on the model Gursona-Tvergaarda-Needleman. Building Review (Przegląd Budowlany) 3 (2012), (in Polish), p. 43-49.
7. Gurson A.L.: Continuum Theory of Ductile Rupture by Void Nucleation and Growth: Part I – Yield Criteria and Flow Rules for Porous Ductile Media. Journal of Engineering Materials and Technology, Transactions of the ASME 99 (1977), pp. 2-15.
8. Tvergaard V.: Influence of Voids on Shear Band Instabilities under Plane Strain Condition, International Journal of Fracture 17 (1981), pp. 389-407.
9. Tvergaard V., Needleman A.: Analysis of The Cup-Cone Fracture in a Round Tensile Bar, Acta Metallurgica 32 (1984), pp. 157-169.
10. Needleman A., Tvergaard V.: An Analysis of The Ductile Rupture in Notched Bars, Journal of the Mechanics and Physics of Solids 32 (1984), pp. 461-490.
11. Cordigliano A., Mariani S., Orsati B.: Identification of Gurson-Tvergaard material model parameters via Kalman filtering technique. I. Theory. International Journal of Fracture, 104 (2000), pp. 349-373.
12. Tvergaard V.: Material failure by void growth to coalescence. Advanced in Applied Mechanics 27 (1989), pp. 83-151.
13. Faleskog J., Gao X., Shih C.F.: Cell model for nonlinear fracture analysis – I. Micromechanics calibration. International Journal of Fracture 89 (1998), pp. 355-373.
14. PN-EN 10002-1:2001 Metallic Materials - Tensile Testing - Part 1: Method of Test at Ambient Temperature.
15. Abaqus 6.10 Analysis User's Manual, Dassault Systèmes, 2010.